Available online at www.sciencedirect.com
SCIENCE DIRECT®
Journal of Magnetic Resonance 168 (2004) 187–193
JMR Journal of Magnetic Resonance
www.elsevier.com/locate/jmr

2D solid state NMR spectral simulation of 3_{10}, α, and π-helices

Sanguk Kim[a] and T.A. Cross[a,b,*]

[a] National High Magnetic Field Laboratory (NHMFL), Institute of Molecular Biophysics, Tallahassee, FL 32310, USA
[b] Department of Chemistry and Biochemistry, Florida State University, Tallahassee, FL 32310, USA

Received 2 September 2003; revised 27 January 2004
Available online 19 March 2004

Abstract

Transmembrane helices are more uniform in structure than similar helices in water soluble proteins. Solid state NMR of aligned bilayer samples is being increasingly used to characterize helical membrane protein structures. Traditional spectroscopic methods have difficulty distinguishing between helices with i to $i+3$ (3_{10}), i to $i+4$ (α), and i to $i+5$ (π) hydrogen bonding topology. Here, we show that resonance patterns in PISEMA spectra simulated for these different helices show unique and striking features. The size and shape of these Polar Index Slant Angle (PISA) wheels, as well as the resonances per turn and clockwise versus counter-clockwise sequential connectivity of the resonances demonstrate how these different helical structures, if present as a uniform structure, will be readily distinguished, and characterized.

Keywords: PISEMA; PISA wheels; 3_{10} Helices; α-Helices; π-Helices

1. Introduction

The membrane environment promotes uniform helical structures through enhanced electrostatic interactions. In water soluble proteins approximately 80% of helices are α-helical and the remaining 20% are 3_{10} helices with π-helices being described infrequently in the Protein Data Bank [1–3]. To date only α-helices have been described in the membrane environment, although π-bulges (an extra amino acid residue in an α-helix) may not be uncommon [4]. However, very few membrane protein structures have been characterized at high resolution. Experimental methods other than complete high resolution structural methods have typically found it difficult to distinguish between helix types [5]. Here, we look at solid state NMR derived Polar Index Slant Angle (PISA) wheels as a new methodology for characterizing and distinguishing between such helices in aligned media.

The backbone intrahelical hydrogen bonding pattern defines these three helical types: 3_{10} has i to $i+3$ hydrogen bonding, α has i to $i+4$ and π has i to $i+5$ hydrogen bonding (Fig. 1). There is a significant range of ϕ, ψ, and ω torsion angles even for regular helices that satisfy this hydrogen bonding pattern. The 3_{10} helix was first described by Donohue [15]. Today, ϕ, ψ torsion angles observed in the Protein Data Bank (PDB) for this helical type show a broad range of values reflecting the short helical segments that typify 3_{10} helical occurrence in water soluble proteins [6]. Mean experimental torsion angles assessed in 1988 [1] were −71° and −18°, and in 1996 [6] were −63° and −17°. A recent computational study [7] has identified an optimal set of values (−68° and −17°) that is close to these experimental mean values. Here, this latter set of torsion angles will be used for the prediction of the NMR spectra for the 3_{10} helix. It should, however, be mentioned that significantly different torsion angles in the vicinity of −54° and −35° have also been described for 3_{10} helices having non-native amino acids [8].

The α-helix was first described by Pauling and collaborators in the early 1950s [9–11]. While the distribution of ϕ, ψ angles in high resolution protein structures is significant, it is much less than for the 3_{10} helices [6]. Mean experimental values calculated in 1988 [1] were −62° and −41° and in 1996 [6] were −65° and −40°. A recent computational effort [7] resulted in

* Corresponding author. Fax: 1-850-644-1366.
E-mail address: cross@magnet.fsu.edu (T.A. Cross).

1090-7807/$ - see front matter © 2004 Elsevier Inc. All rights reserved.
doi:10.1016/j.jmr.2004.02.009

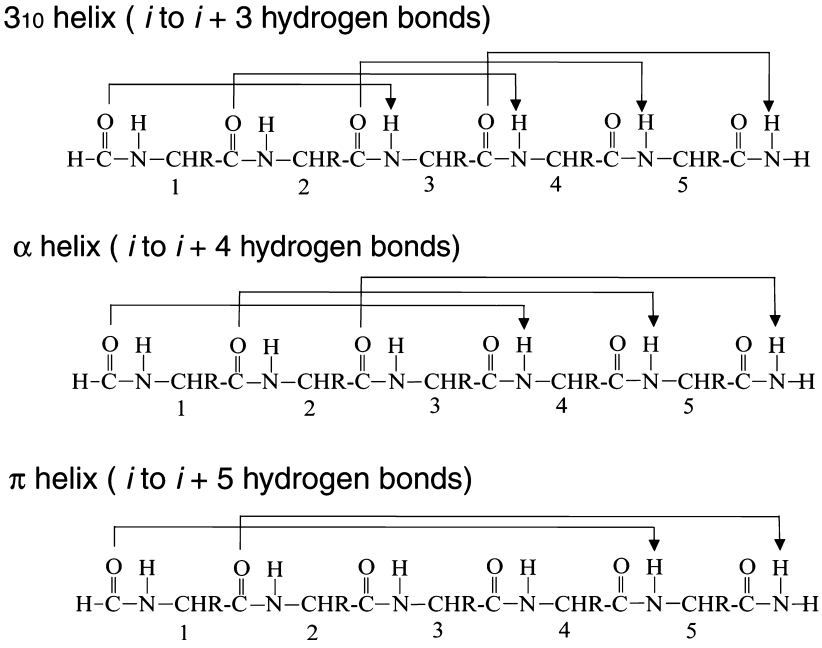

Fig. 1. Helical conformations and their hydrogen bond patterns. Lines and arrows denote hydrogen bonds.

optimal values of −67° and −40°. Consistent with our earlier spectral simulations of the α-helix [12,13] we have continued to use ϕ, ψ angles of −65° and −40° here.

The π-helix was first described by Low and Baybutt [14] followed soon after by two additional studies [15,16] resulting in a characteristic model with torsion angles of −57° and −70°. Weaver [2] identified 10 π-helices in the PDB and Fodje and Al-Karadaghi [3] identified 104 π-helices in 932 high resolution structures. Hence, these helices are not as rare as once thought. However, 73% of these helices have just two i to $i+5$ type hydrogen bonds and an additional 17% of the structures have just three of these characteristic hydrogen bonds. The mean torsion angles are −76° and −41° for these structures, quite different from the early models. However, these are not regular helical structures with a single amino acid being the repeat unit. For instance, the mean torsion angle values for residues 4 and 5 in the π-helices are −96°, −26°, and −97°, −51° [3]. Furthermore, there is a characteristic amino acid distribution among the helical sites. Since the effort being reported here is on recognizing regular helical structures, such as those that might occur in the low dielectric environment of the membrane, we have chosen to use the torsion angles from the helical models (−57°, −70°) of π-helices.

Experimental discrimination between helical types has been difficult to accomplish, because of the difficulties in achieving quantitative experimental measurements and the frequent presence of conformational distributions in sample preparations [5]. Circular dichroism of 3_{10} helices shows a characteristic signature spectrum [17,18], but the characteristic molar ellipticities are weak and overlap with the characteristic features for an α-helix. ESR measurements with doubly spin labeled samples were some of the first experiments used to characterize 3_{10} helices, but even here there has been ambiguity [19]. Solution NMR displays no unique distances that are absolutely characteristic of 3_{10} helices and therefore without a very substantial dataset, solution NMR provides an ambiguous characterization. However, with detailed datasets or in combination with hydrogen-exchange data it is possible to characterize 3_{10} helices well [6,20]. Magic angle spinning solid state NMR through chemical exchange experiments has also been used to characterize 3_{10} helices in the presence of α-helices [5].

Recent results from X-ray crystallography and solid state NMR suggest that many helices in a membrane environment may be more regular than what is typically observed in water soluble proteins [4,13,21]. The scarcity of water and the low dielectric environment of the bilayer intersiticies combine for the explanation of this result. The lack of water results in fewer opportunities to destabilize the helical hydrogen bonds. In water soluble protein helices 36% of the backbone carbonyl sites have more than one hydrogen bond, the second of which is typically water [22]. The low dielectric environment in the membrane results in a strengthening of intrahelical hydrogen bonds. Indeed, hydrogen bond distances in both high resolution crystal structures (<2.0 Å resolution) and in solid state NMR derived structures appear to be approximately 0.1 Å shorter in the membrane environment [21] than average helical hydrogen bonds in water soluble proteins. This is consistent with helical

hydrogen bonds that do not share their carbonyl oxygen with other hydrogen bond donors [22]. Furthermore, the dispersion of ϕ, ψ torsion angles is greatly reduced in these high resolution membrane protein structures compared to high resolution water soluble helices. As a result it is possible to observe PISA wheels [12,23] in solid state NMR PISEMA spectra that correlate anisotropic ^{15}N chemical shift with ^{15}N–^{1}H dipolar interactions [24].

Solid state NMR spectroscopy of uniformly aligned samples has been used to characterize membrane peptide and protein structures (PDB #1MAG [25,26]; PDB #1NYJ [27]; PDB #1CEK [28]; PDB #1PJD [29]; PDB #1PJE, Opella et al. [28] deposited; PDB #1MZT, Marassi and Opella [23] deposited). Orientational restraints derived from PISEMA spectra [24] correlate the anisotropic ^{15}N chemical shift and ^{15}N–^{1}H dipolar interactions. The observed resonance frequencies reflect the $P_2(\cos\theta)$ orientation dependence of these spin interactions with respect to the direction of the bulk magnetic field, B_0. Since these tensors are fixed with respect to the molecular frame by well characterized angles [30–32] the observed frequencies restrain the orientation of individual amide molecular frames with respect to B_0. In 2000 it was recognized [12,23] in PISEMA spectra that α-helices give rise to resonance patterns that were reminiscent of helical wheels having 3.6 resonances per turn. Here, patterns for 3_{10} and π-helices are compared to α-helical spectral simulations. Previously, examples of these patterns have been published [33].

2. Results and discussion

The 3_{10} helix has 3.2, the α-helix 3.6 and the π-helix 4.3 residues per turn, as shown in Fig. 2 at the bottom. This corresponds to 112°, 100°, and 84° rotation per residue about the helical wheel, respectively. All of the helices are right-handed, as shown by the helical wheels, and for each case the helical repeat is a single amino acid residue. However, they are each characterized by a different tilt angle of the peptide plane with respect to the helical axis. It is possible to show this by correlating the features of local helical structure with torsion angles (Fig. 3). Here, the peptide plane tilt angle (δ) is displayed as contour lines in this Ramachandran diagram. Note that through the center of this plot is a line for $\delta = 0°$, indicating that for this set of ϕ, ψ torsion angles the peptide plane is parallel to the helical axis. Above this line the positive values of δ indicate peptide planes where the carbonyl oxygens are tilted away from the helical axis and below this line the negative values indicate that the carbonyl oxygens are tilted in toward the helix axis. Therefore, both in Fig. 2 at the top and in Fig. 3 it can be seen that the 3_{10} helix is typically characterized by peptide plane tilt values greater than that of an α-helix and the π-helix has a slightly negative δ value.

In Fig. 2 PISEMA spectra are predicted for each helix tilted with respect to B_0 by 30°. For these simulations that generate PISA wheels, just one of the dipolar transitions is displayed. Here, the transition that generates a right-handed or clock-wise pattern for the α-helix is chosen. The same dipolar transition has been used in the other spectral simulations. The 3_{10} helix, which also has a positive δ value displays a clock-wise pattern of resonances. However, the π-helix has a slightly negative δ value and this leads to a counter clock-wise pattern or resonances. The number of resonances per turn in the PISA wheels is different for these three helices, 3.2, 3.6, and 4.3, reflecting the number of α-carbons per turn in the helical wheels.

In Fig. 4 PISA wheels for each of the helical types are generated for tilt angles of the helix axis with respect to B_0 of 8°, 18°, 38°, 58°, 78°, and 90° (τ). While the 'center of mass' position of the PISA wheel in the spectrum is the same for all helical types at a given τ, shapes of the PISA wheels are very different for the three helical types. The resonances for a given PISA wheel are spread out in spectral space because these two spin interactions are not colinear. If, the spin interaction tensors were colinear the variations in chemical shift–dipolar interactions would be restricted to a line segment superimposed on the line connecting the PISA wheel's 'center of mass' for different τ (dashed line in Fig. 4). The angle between the N–H vector (the dipolar interaction axis) and the σ_{33} tensor element of the chemical shift tensor is 17° [12,32]. The asymmetry of the chemical shift tensor further complicates the PISA wheels at high helix tilt angles ($\tau > 50°$).

The size of the PISA wheels is largely dependent on the tilt angle of the peptide plane with respect to the helical axis (δ). For ϕ, ψ angles of −68° and −17° the δ value is 18.9° and the PISA wheels are very large. For a helix tilt (τ) of just 18° the ^{15}N–^{1}H dipolar interaction will range from 2.3 to 10 kHz and the chemical shift from 200 to 145 ppm. For the π-helix having torsion angles of −57° and −70° and a δ value of −2.2° the dipolar interaction ranges from 8.0 to 9.7 kHz, just 22% of the range for the 3_{10} helix. Indeed, this pattern collapses at $\delta = 0°$ as it inverts from a clock-wise to counter clock-wise pattern. This correlation of the PISA wheel size with δ is qualitative and, while it holds up for these three samples of ϕ, ψ space for the dipolar interaction, the chemical shift interaction shows a larger range for the π-helix (45 ppm) than for the α-helix (23 ppm), which has a δ value of 11.8°.

The fact that α-helical structures are more uniform in a membrane environment suggests that other regular helical structures will be more uniform in a membrane environment than they are in water soluble proteins and consequently it can be anticipated that wheel-like

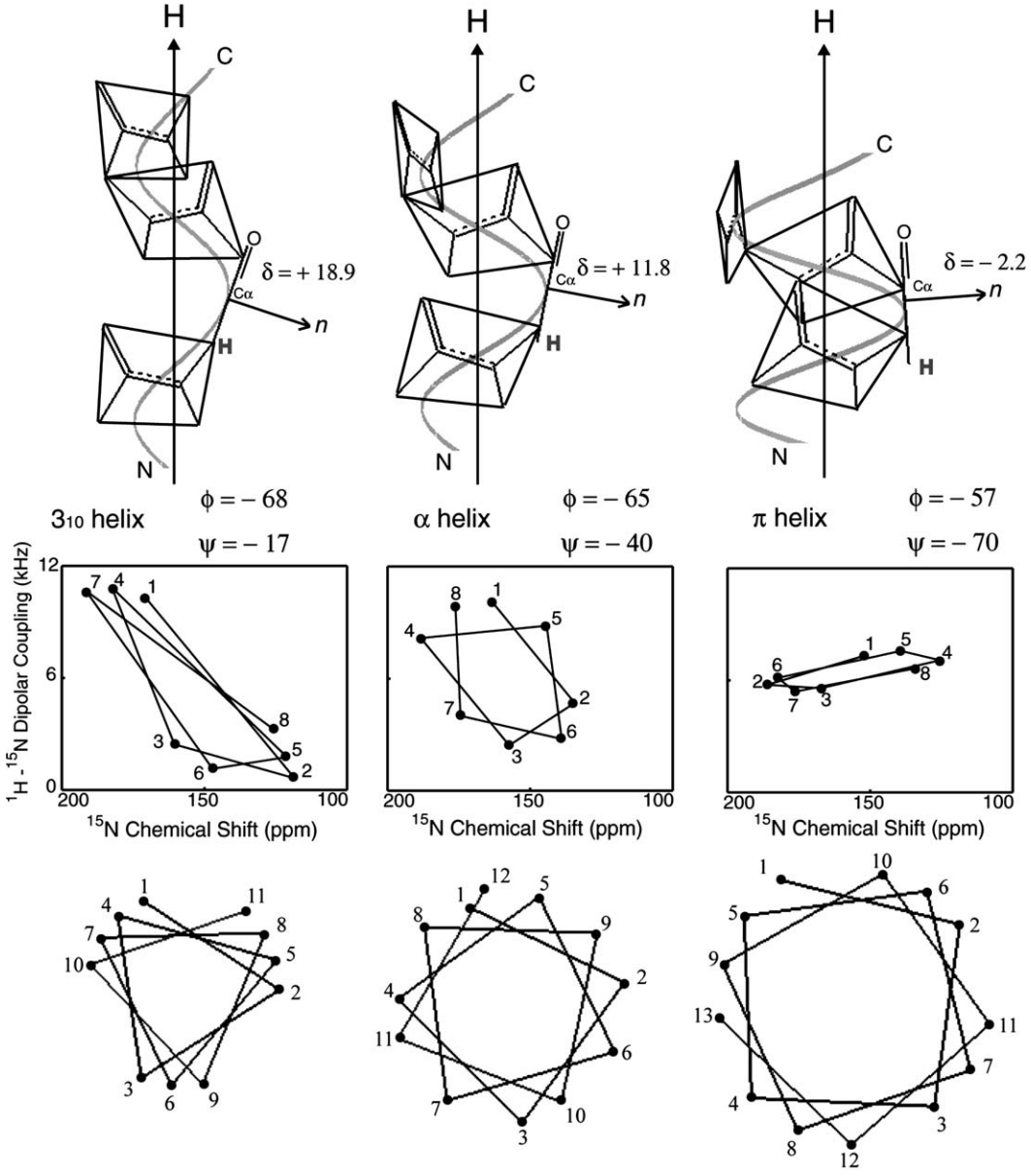

Fig. 2. The relationship between structure, helical wheel projections, and PISA wheel patterns for 3_{10}, α, and π-helices. The size and shape of the PISA wheels are influenced by the magnitude of the δ angle. The sign of δ angle changes the rotational direction about the PISA wheel for i to $i+1$ resonance patterns. Note that the same scale of bond lengths is used for the helical wheel projections so that their relative size is illustrated. Helical tilt (τ) of 30° is used for the simulation of PISEMA spectra.

patterns can be expected for 3_{10} and π-helices, just as they are observed for α-helices. The remarkable sensitivity of the PISA wheel's shape to ϕ, ψ angles provides a potential mechanism for identifying, and characterizing these different helical types if they are present in the membrane environment. At the same time, this remarkable sensitivity could blur the PISA wheel pattern if there is non-uniformity among the set of ϕ, ψ angles. As previously shown, low resolution crystal structures (>2.0 Å resolution) cannot be used for PISA wheel predictions, whereas higher resolution (<2.0 Å resolution) structures show clear PISA wheels due to the improvement in the atomic coordinates [21,34]. The high resolution membrane protein structures show remarkable homogeneity in the α-helical torsion angles except at the site of a kink, π-bulge, etc. Here, we have also assumed uniform torsion angles for 3_{10} and π-helices, since the same set of forces that have regularized α-helices, will be present to regularize 3_{10} and π-helices. This is, however, not to say that ideal PISA wheels are to be expected. There will be deviations from ideality due, not only from small variations in ϕ, ψ angles, but also due to variations in chemical shift tensor element magnitudes, and tensor orientations. These tensor effects have pre-

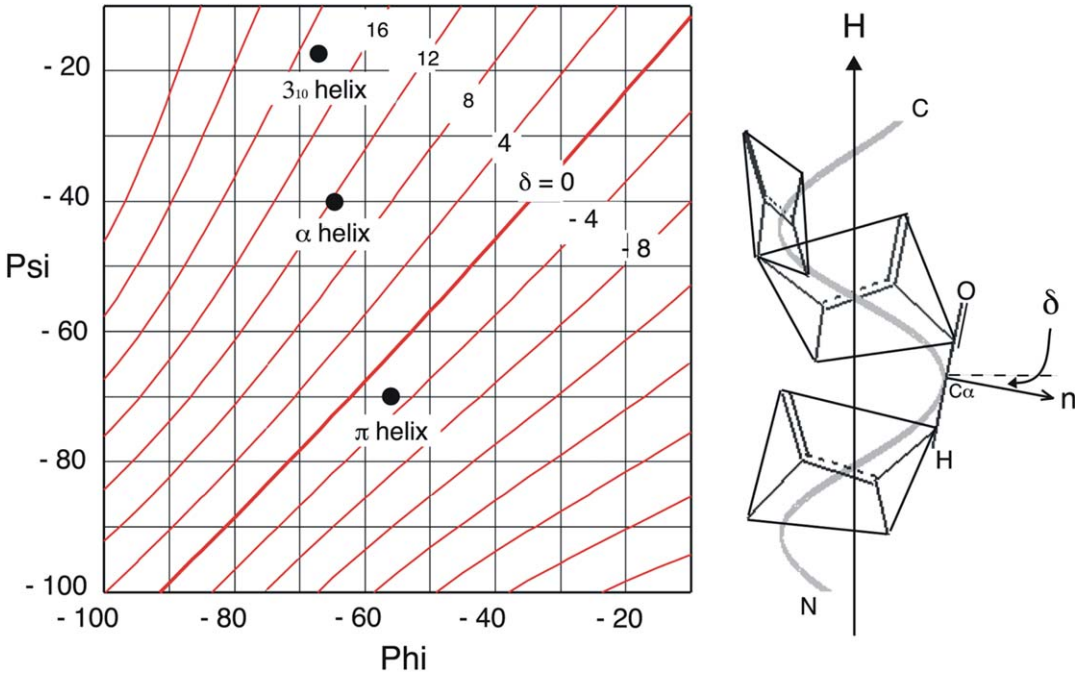

Fig. 3. Ramachandran–delta plot. Peptide plane tilt angles to the helical axis (δ) are diagramed as a function of ϕ, ψ torsion angles from uniform helical models. The δ angles are calculated from the angle between the helical axis and the peptide plane as previously described [21].

viously been described and are independent of the type of helix [12].

While there is no doubt from the present membrane protein database that α-helices are the dominant helical structure in the membrane environment, there may be reasons to expect other helical conformations. For instance, the 3_{10} helix, which typically has a larger δ value than the α-helix, may present better opportunities for involving the protein backbone in functional chemistry than would the α-helical geometry. While 36% of backbone carbonyls in water soluble protein helices are involved in bifurcated hydrogen bonds [22] it is unlikely that this is the case in a transmembrane environment. The percentage of hydrophilic sidechains is greatly reduced [35] and water is scarce. As a result, the average δ values may be less for transmembrane α-helices and most carbonyl oxygens will be largely secluded from participating in any chemistry other than intrahelical hydrogen bonds. The recent high resolution structure of the transmembrane peptide, M2-TMP in a tetrameric bundle [27] supports this notion with average ϕ, ψ torsion angles of −61° and −46° corresponding to a δ value of 8° instead of the PDB mean values of −65° and −40° [6] corresponding to $\delta = 12°$. A 3_{10} helix is not able to seclude its carbonyl oxygens to the same extent with $\delta = 19°$ and potentially there may be a chemical and functional need for more than the occasional backbone carbonyl oxygen, such as that produced by a π-bulge. A 3_{10} helix would probably not be exposed to the lipid environment, but might be present in the membrane protein interior, e.g., surrounded by an α-helical bundle.

PISA wheels, their size and shape as well as the number of resonances per turn and the handedness of the resonance pattern all contribute to a unique sensitivity for the type of helix and their specific structural details. The "center of mass" of the resonance pattern defines the tilt of helical axis with respect to B_0 and the bilayer normal independent of the helix type and therefore does not complicate the interpretation of helix type. If structurally uniform 3_{10} or π-helices are present in membrane proteins, PISEMA experiments should be able to easily recognize the helix type and, as with α-helices, unambiguously characterize the molecule structure.

3. Methods

3.1. PISEMA spectra simulations

PISEMA spectra are simulated from the coordinates of helices built as uniform 3_{10} ($\phi = -68$, $\psi = -17$) $\alpha - (\phi = -65, \psi = -40)$, and $\pi - (\phi = -57, \psi = -70)$ helices with the InsightII Biopolymer package (Accelys). The theoretical detail of the simulation was described previously [12,13]. Briefly, uniform chemical shift tensors ($\sigma_{11} = 31.3$, $\sigma_{22} = 55.2$, $\sigma_{33} = 201.8$ ppm) and a dipolar magnitude of 10.735 kHz were used for the simulations. The values take into account modest local dynamics of the peptide planes. A typical relative orientation (θ) between the σ_{33} chemical shift tensor element and $\nu_{\|}$ of the dipolar tensor equal to 17° was used

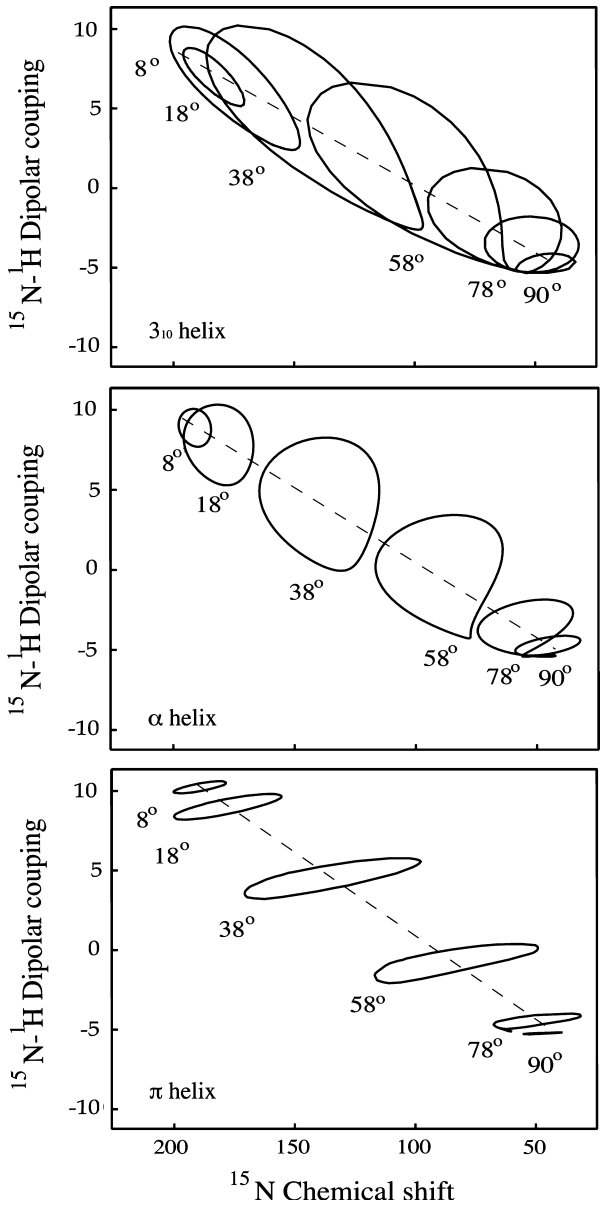

Fig. 4. PISA wheel patterns of 3_{10}, α, and π-helices drawn for one of the dipolar transitions using various helical tilt angles (τ). The 'center of mass' for each PISA wheel characterizes the tilt of the helix axis (τ) with respect to B_0 independent of the helix types. A line through the 'center of mass' is shown in each panel. The size, shape, and rotational direction of the patterns are influenced by the peptide plane tilt with respect to the helical axis (δ). Note that the simulations are done using average values of tensor elements and a dipolar magnitude.

[12], consistent with previous experimental characterizations [31,32]. All ^{15}N chemical shifts are relative to the resonance for a saturated solution of $^{15}NH_4NO_3$ at 0 ppm.

Acknowledgments

This work was supported by the National Science Foundation, MCB 02-35774, and the work was performed at the National High Magnetic Field Laboratory supported by the National Science Foundation Cooperative Agreement DMR 00-84173 and the State of Florida.

References

[1] D.J. Barlow, J.M. Thornton, Helix geometry in proteins, J. Mol. Biol. 201 (1988) 601–619.
[2] T.M. Weaver, The π-helix translates structure into function, Protein Sci. 9 (2000) 201–206.
[3] M.N. Fodje, S. Al-Karadaghi, Occurrence, conformational features, and amino acid propensities for the π-helix, Protein Eng. 15 (2002) 353–358.
[4] H. Luecke, B. Schobert, H.-T. Richter, J.-P. Cartailler, J.K. Lanyi, Structure of bacteriorhodopsin at 1.55 Å resolution, J. Mol. Biol. 291 (1999) 899–911.
[5] H.W. Long, R. Tycko, Biopolymer conformational distribution from solid state NMR: α-helix and 3_{10} helix contents of a helical peptide, J. Am. Chem. Soc. 120 (1998) 7039–7048.
[6] L.J. Smith, K.A. Bolin, H. Schwalbe, M.W. MacArthur, J.M. Thornton, C.M. Dobson, Analysis of main chain torsion angles in proteins: prediction of NMR coupling constants for native and random coil conformations, J. Mol. Biol. 255 (1996) 494–506.
[7] Y.D. Wu, Y. Zhao, A theoretical study on the origin of cooperativity in the formation of 3_{10} and α-helices, J. Am. Chem. Soc. 123 (2001) 5313–5319.
[8] R. Gratias, R. Konat, H. Kessler, M. Crisma, G. Valle, A. Polese, F. Formaggio, C. Toniolo, Q.B. Broxterman, J. Kamphuis, First step towards the quantitative identification of peptide 3_{10}-helix conformation with NMR spectroscopy: NMR and X-ray diffraction structural analysis of a fully-deuterated 3_{10}-helical peptide standard, J. Am. Chem. Soc. 120 (1998) 4763–4770.
[9] L. Pauling, R.B. Corey, Two hydrogen-bonded spiral configurations of the polypeptide chain, J. Am. Chem. Soc. 72 (1950) 5349.
[10] L. Pauling, R.B. Corey, Atomic coordinates and structure factors for two helical configurations of polypeptide chains, Proc. Natl. Acad. Sci. USA 37 (1951) 235–240.
[11] L. Pauling, R.B. Corey, H.R. Branson, The structure of proteins: two hydrogen-bonded helical configurations of the polypeptide chain, Proc. Natl. Acad. Sci. USA 37 (1951) 205–211.
[12] J. Wang, J. Denny, C. Tian, S. Kim, Y. Mo, F. Kovacs, Z. Song, K. Nishimura, Z. Gan, R. Fu, J.R. Quine, T.A. Cross, Imaging membrane protein helical wheels, J. Magn. Reson. 144 (2000) 162–167.
[13] J. Wang, S. Kim, F. Kovacs, T.A. Cross, Structure of the transmembrane region of the M2 protein H^+ channel, Protein Sci. 10 (2001) 2241–2250.
[14] B.W. Low, R.B. Baybutt, The π-helix: a hydrogen bonded configuration of the polypeptide chain, J. Am. Chem. Soc. 74 (1952) 5806–5807.
[15] J. Donohue, Hydrogen bonded helical configurations of the polypeptide chain, Proc. Natl. Acad. Sci. USA 39 (1953) 470–478.
[16] B.W. Low, H.J. Grenville-Wells, Generalized mathematical relationships for polypeptide chain helices. The coordinates of the π-helix, Proc. Natl. Acad. Sci. USA 39 (1953) 785–802.
[17] C. Toniolo, A. Polese, F. Formaggio, M. Crisma, J. Kamphuis, Circular dichroism spectrum of a peptide 3_{10}-helix, J. Am. Chem. Soc. 118 (1996) 2744–2745.
[18] Z. Biron, S. Khare, A.O. Samson, Y. Hayek, F. Naider, J. Anglister, A monomeric 3_{10}-helix is formed in water by a 13-residue peptide representing the neutralizing determinant of HIV-1 on gp41, Biochemistry 41 (2002) 12687–12696.
[19] M.L. Smythe, C.R. Nakaie, G.R. Marshall, α-Helical versus 3_{10}-helical conformation of alanine-based peptides in aqueous solu-

tion: an electron spin resonance investigation, J. Am. Chem. Soc. 117 (1995) 10555–10562.
[20] G.L. Millhauser, C.J. Stenland, P. Hanson, K.A. Bolin, F.J.M. van de Ven, Estimating the relative populations of 3_{10}-helix and α-helix in ala-rich peptides: a hydrogen exchange and high field NMR study, J. Mol. Biol. 267 (1997) 963–974.
[21] S. Kim, T.A. Cross, Uniformity, ideality, and hydrogen bonds in transmembrane α-helices, Biophys. J. 83 (2002) 2084–2095.
[22] E.N. Baker, R.E. Hubbard, Hydrogen bonding in globular proteins, Prog. Biophys. Molec. Biol. 44 (1984) 97–179.
[23] F.M. Marassi, S.J. Opella, A solid-state NMR index of helical protein structure and topology, J. Magn. Reson. 144 (2000) 150–155.
[24] C.H. Wu, A. Ramamoorthy, S.J. Opella, High resolution heteronuclear dipolar solid-state NMR spectroscopy, J. Magn. Reson. A 109 (1994) 270–272.
[25] R.R. Ketchem, W. Hu, T.A. Cross, High resolution conformation of gramicidin a in a lipid bilayer by solid-state NMR, Science 261 (1993) 1457–1460.
[26] R.R. Ketchem, B. Roux, T.A. Cross, High-resolution polypeptide structure in a lamellar phase lipid environment from solid-state NMR derived orientational constraints, Structure 5 (1997) 1655–1669.
[27] K. Nishimura, S. Kim, L. Zhang, T.A. Cross, The closed state of a H^+ channel helical bundle: combining precise orientational and distance restraints from solid state NMR, Biochemistry 41 (2002) 13170–13177.
[28] S.J. Opella, F.M. Marassi, J.J. Gesell, A.P. Valente, Y. Kim, M. Oblatt-Montal, M. Montal, Structures of the M2 channel-lining segments from nicotinic acetylcholine and NMDA receptors by NMR spectroscopy, Nat. Struct. Biol. 6 (1999) 374–379.
[29] K.G. Valentine, S.F. Liu, F.M. Marassi, G. Veglia, S.J. Opella, F.X. Ding, S.H. Wang, B. Arshava, J.M. Becker, F. Naider, Structure and topology of a peptide segment of the 6 transmembrane domain of the *saccharomyces cerevisiae* α-factor receptor in phospholipid bilayers, Biopolymers 59 (2001) 243–256.
[30] G.S. Harbison, L.W. Jelinski, R.E. Stark, D.A. Torchia, J. Herzfeld, R.G. Griffin, ^{15}N chemical shift and ^{15}N–^{13}C dipolar tensors for the peptide bond in [1-^{13}C]Glycyl[^{15}N]glycine hydrochloride monohydrate, J. Magn. Reson. 60 (1984) 79–82.
[31] T.G. Oas, C.J. Hartzell, F.W. Dahlqust, G.P. Drobny, The carbonyl ^{13}C chemical shift tensors of 5 peptides determined from ^{15}N dipole-coupled chemical-shift powder patterns, J. Am. Chem. Soc. 109 (1987) 5956–5962.
[32] Q. Teng, M. Iqbal, T.A. Cross, Determination of the ^{13}C chemical shift and ^{14}N electric field gradient tensor orientations with respect to the molecular frame in a polypeptide, J. Am. Chem. Soc. 114 (1992) 5312–5321.
[33] M.F. Mesleh, S.J. Opella, Dipolar waves as NMR maps of helices in proteins, J. Magn. Reson. 163 (2003) 288–299.
[34] T.A. Cross, S. Kim, J. Wang, J.R. Quine, From topology to high resolution membrane protein structures, in: S.R. Kiihne, H.J.M. de Groot (Eds.), Proceedings of the Workshop on the Future of Solid State NMR in Biology, Kluwer Academic Publishers, Dordrecht, 2001, pp. 55–70.
[35] M. Eilers, A.B. Patel, W. Liu, S.O. Smith, Comparison of helix interactions in membrane and soluble α-bundle proteins, Biophys. J. 82 (2002) 2720–2736.